JOURNAL OF APPLIED PHYSICS **105**, 104305 (2009)

Chemically mediated diffusion of *d*-metals and B through Si and agglomeration at Si-on-Mo interfaces

Tim Tsarfati,[1,a)] Erwin Zoethout,[1] Robbert van de Kruijs,[1] and Fred Bijkerk[1,2]
[1]*FOM Institute for Plasma Physics Rijnhuizen, 3430 BE Nieuwegein, The Netherlands*
[2]*MESA+ Institute for Nanotechnology, University of Twente, 7522 NB Enschede, The Netherlands*

(Received 18 February 2009; accepted 2 April 2009; published online 18 May 2009)

Chemical diffusion and interlayer formation in thin layers and at interfaces is of increasing influence in nanoscopic devices, such as nanoelectronics and reflective multilayer optics. Chemical diffusion and agglomeration at interfaces of thin Ru, Mo, Si, and B_4C layers have been studied with x-ray photoelectron spectroscopy, cross section electron energy loss spectroscopy, high-angle annular dark field scanning transmission electron microscopy, and energy dispersive x-ray in relation to observations in Ru-on-B_4C capped Mo/Si multilayers. Rather than in the midst of the Si layer, silicides and borides are formed at the Si-on-Mo interface front, notably $RuSi_x$ and MoB_x. The interface apparently acts as a precursor for further chemical diffusion and agglomeration of B, Ru, and also other investigated *d*-metals. Reversed "substrate-on-adlayer" interfaces can yield entirely suppressed reactivity and diffusion, stressing the influence of surface free energy and the supply of atoms to the interface via segregation during thin layer growth. © *2009 American Institute of Physics*. [DOI: 10.1063/1.3126497]

I. INTRODUCTION

The morphology of layer growth on a dissimilar substrate layer is affected by the lattice mismatch, the chemical reactivity, and the surface free energy difference.[1,2] In this paper we characterize the influence of these factors by considering nanometer thin Ru, Mo, Si, and B_4C substrate and adsorbate layers to cover a wide range of interface characteristics. Ru does not readily react with Mo and the two transition metals have comparable lattice spacings and surface free energies that are very different from Si and B_4C. Mo forms a relatively stable silicide interface with Si,[3] while Ru and some other *d*-metals diffuse into a Si substrate layer without significant reactivity.[4] B_4C dissociates upon deposition and readily forms borides with Mo and Ru, while carbides are only kinetically favored with Mo and Si.[3] All materials involved are considered both as ad- and substrate layer to study the effect of dissociative B_4C deposition as observed by Nedelcu *et al.*,[3] and the surface free energy driven intermixture (segregation) on the adsorbate/substrate dependency for compound formation. Layer and interface growth and compound formation can be optically studied in multilayer coatings that act as artificial Bragg crystals. Reflective multilayer x-ray optics are also of increasing importance for applications in astronomy, medicine, and next generation lithography.

For extreme UV lithography (EUVL) ($\lambda = 13.5$ nm), high contrast Mo/Si multilayers with individual layer thicknesses of 3–4 nm are applied as condenser, illuminator, and projection optics. To protect the reflecting mirror surface against photo induced oxidation and the resulting decrease in reflectivity, a capping layer is applied on top of the multilayer,[5] with Ru as a common reference material.[6,7] Cap thickness and intermixture with the layers beneath strongly influence the overall reflection and the protection that the cap offers. We relate our characterization of the interlayers between B_4C, Ru, Mo, and Si to the application of a B_4C diffusion barrier layer between the Ru and subsurface Si. This could reduce the overall intermixing and limit subsequent reflection loss, as proposed by Bâjt *et al.*[7]

II. EXPERIMENTAL DETAILS

The layers have been grown onto natively oxidized super polished Si (100) substrates that are precoated with Si in an electron-beam physical vapor deposition setup with a base pressure of 1×10^6 Pa.[8] This deposition technique was used for Si, B_4C, Mo, and Ru to limit direct implantation of high energy atoms that might occur using higher adatom energy deposition techniques such as magnetron sputtering. Quartz crystal oscillator mass balances and *in situ* C $K\alpha$ x-ray reflectometry are used for layer thickness control. A flux-shaping mask is used to deposit the B_4C diffusion barrier with a lateral layer thickness gradient from 0.4 to 5.0 nm,[9,10] before depositing the Ru capping layer.

A Thermo Theta Probe monochromated Al $K\alpha$ x-ray photoelectron spectroscopy (XPS) setup with ion gun was used for sputtering and immediate subsequent on spot analysis of the in-depth material distribution and compound formation. The penetration and possible ion mixing depths of the used 0.5 keV Ar^+ sputter ions at 45° incidence are ~1.6 nm in Si, ~1.3 nm in B_4C, and ~0.7 nm in *d*-metals such as Mo and Ru.[11] Considering the ~0.7 nm inelastic mean free path of the photoelectrons,[12] the calculated ion mixing components are minor to moderate.

Differences in sputter efficiency and electron escape depths for the different materials result in underestimation of the Si content in the multilayer. This can result in early detection of subsurface elements during depth profiling, i.e., an apparent layer front shift to the surface. Thin layer systems

[a)]Electronic mail: t.tsarfati@rijnhuizen.nl.

 © 2009 American Institute of Physics

Downloaded 07 Sep 2010 to 130.89.22.124. Redistribution subject to AIP license or copyright; see http://jap.aip.org/about/rights_and_permissions

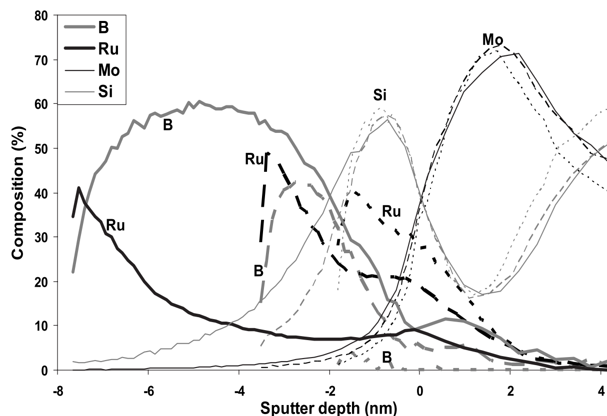

FIG. 1. XPS sputter depth profiles of three $Ru/B_4C/Si/(Mo/Si)$ multilayers with 5.0 nm (solid line), 1.7 nm (dashed line), and 0.4 nm (dotted line) thick B_4C diffusion barriers.

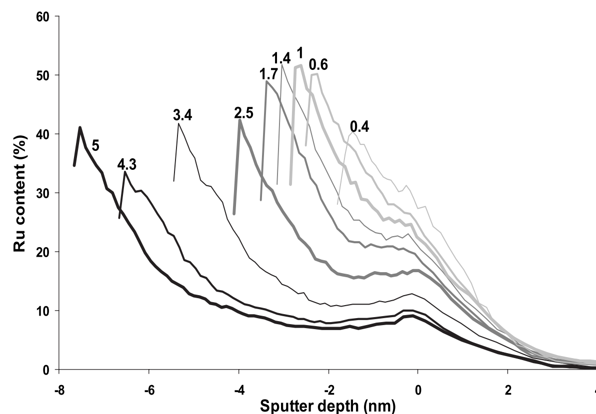

FIG. 2. In-depth Ru content in atomic percent for various B_4C barrier layer thicknesses (labeled in nanometers) as determined by XPS sputter depth profiling.

thus appear more smeared out than they are. Considering that the XPS probing depth is considerably larger than the range of ion-beam induced chemistry, the in-depth modulation of electron binding energies, i.e., XPS peak shifts, can give a good indication of in-depth chemical states.

The depth scale in the graphs shown in this study is determined from the deposited layer thicknesses and periodicity in the multilayer as established by quartz microbalances and *in situ* reflection measurements. Differences in sputter efficiency and electron escape depths for the different materials that result in underestimation of the Si content in the multilayer are not of influence in the presented results, considering our focus on the surface composition and not on multilayer periodicity.

Cross section electron energy loss spectroscopy (CS-EELS), high-angle annular dark field scanning transmission electron microscopy (HAADF-STEM) and energy dispersive x-ray (EDX) analysis were performed with a FEI Tecnai F30ST, operated at 300 kV. The samples were prepared by focused ion beam (FIB) using a FIB2000. This procedure damages the upper ~20 nm of the sample. The sample is first analyzed with a sample thickness of ~100 nm and ion-beam damage on both sides. Further thinning to <80 nm was achieved with low-energy ions.

III. RESULTS AND DISCUSSION

Figure 1 shows the sputter depth profiles of three $Ru/B_4C/Si/(Mo/Si)$ multilayers with B_4C layer thicknesses of 5.0 nm (solid line), 1.7 nm (dashed line), and 0.4 nm (dotted line). The Ru and Si layers are kept at constant 1.5 and 2.5 nm thicknesses, respectively.[4] The profiles are matched to the multilayer periods, with the top Si-on-Mo interface defined at 0.0 nm sputter depth.

The smearing out of Mo when thicker B_4C diffusion barriers are applied on top can be attributed to some loss of depth resolution. The Si appears to diffuse upward into the on top B_4C due to its lower surface free energy.[13–15] We do not observe a shift in the Si 2*p* electron binding energy (BE) from its elemental value of 99.3 eV. This suggests that recombination of atomically deposited B_4C occurs at the Si substrate layer and no kinetically unfavorable SiB_x and SiC_x are formed. To consider the in-depth Ru distribution in more detail, it has been plotted separately for all investigated underneath B_4C diffusion barrier thicknesses in Fig. 2, with the abscissa similar to Fig. 1.

Observed from the Ru surface, all depth profiles in Fig. 2 show a similar exponential decay in Ru content over a depth of several nanometers, as would be expected for a layered structure. The Ru diffuses through both the B_4C and the Si, agglomerating at the Si-on-Mo interface as defined at 0 nm depth. Within the investigated range of B_4C barrier thicknesses, none of the B_4C diffusion barriers is observed to completely inhibit Ru diffusion. The increasing Ru residue below the B_4C layer for decreasing B_4C layer thickness has been confirmed using Auger electron spectroscopy depth profiling.[7] Ru, Rh, Y, Nb, and Ir also diffuse through a Mo and Si layer to agglomerate at the Si-on-Mo interface, generalizing the observations for a range of *d*-metals.[4] To verify that the observations are not a result of lateral Ru-on-B_4C growth inhomogeneity, Fig. 3 shows an atomic force microscopy (AFM) image of a Ru/B_4C capped multilayer surface when a 2.0 nm thick B_4C diffusion barrier is applied.

The AFM image in Fig. 3 reveals a 0.1 nm rms and 0.57 nm peak-to-valley roughness, indicating that Ru-on-B_4C growth and the observed diffusion do not increase roughness

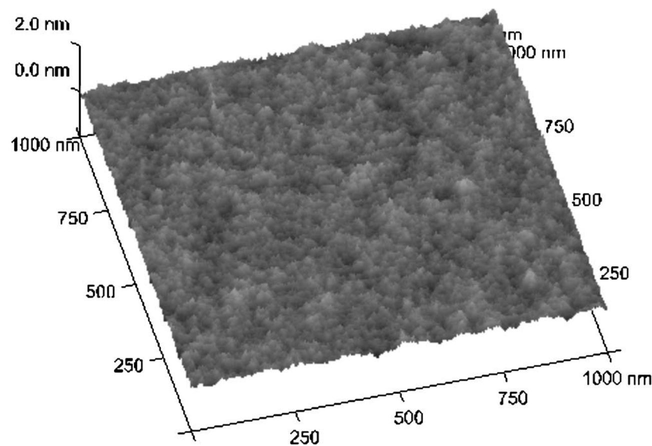

FIG. 3. AFM image of a Ru capped multilayer with a 2.0 nm thick B_4C diffusion barrier.

Downloaded 07 Sep 2010 to 130.89.22.124. Redistribution subject to AIP license or copyright; see http://jap.aip.org/about/rights_and_permissions

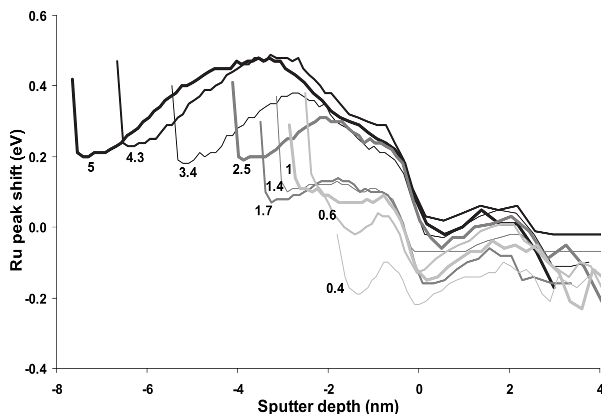

FIG. 4. Ru $3d_{5/2}$ peak deviation from it elemental value of 280.0 eV BE for various B_4C barrier layer thicknesses (labeled in nanometers) as established by in-depth XPS analysis.

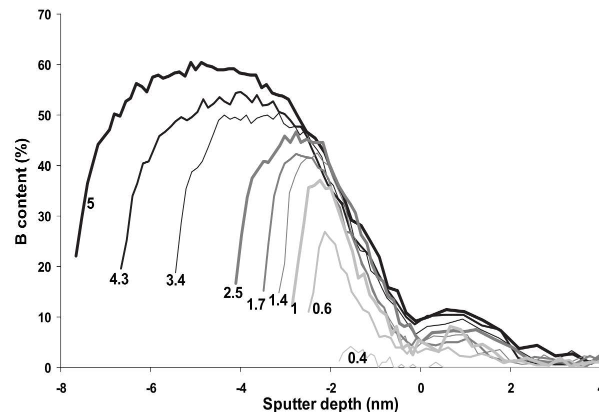

FIG. 5. In-depth B distribution for various B_4C barrier layer thicknesses (labeled in nanometers) as established by XPS sputter depth profiling.

compared to Ru/Mo/Si/(Mo/Si) multilayers, for which Ru agglomeration at the Si-on-Mo interface front was also visible in 0.5 and 0.25 keV Ar^+ depth profiles.[4] The Ru agglomeration persisted or even increased after 48 h anneal at 300 °C, implying that the agglomeration is a thermodynamically preferred configuration.

Figure 4 shows the Ru $3d_{5/2}$ in-depth peak shift from its elemental value in reference to the Fermi level, giving an indication of the chemical state and compound formation. The in-depth Ru $3d_{5/2}$ BE modulation up to 0.5 eV in the 4.3 and 5.0 nm thick B_4C layers cannot be attributed to oxidation as is the case at the surface, since no subsurface oxygen is observed in XPS. A coinciding B 1*s* BE increase from 188.0 to 188.6 eV suggests RuB formation at the cost of B_4C decomposition. The C 1*s* peak appears to shift from 282.0 to 282.8 eV, suggesting a transition from carbide (B_4C) in the direction of the elemental value of 284.5 eV. Toward the Si/Mo interface, the Si 2*p* BE increase in 0.3 eV suggests silicide formation. The Mo $3d_{5/2}$ peak at 227.8 eV BE excludes neither elemental Mo nor a silicide. At the Si/Mo interface, the decrease in Ru $3d_{5/2}$ BE observed in Fig. 4 suggests Ru_2Si_3 formation. This means that the Ru agglomeration, as observed in Fig. 2, coincides and likely is a result of Ru_2Si_3 formation at the Si/Mo interface, which would sustain Ru migration. Toward the Si/Mo interface, a change in the nearest neighbor distance and/or formation of Mo silicides could accommodate Ru_2Si_3 formation. With $E_{act} \approx 130$ kJ/mol, $MoSi_2$ could be an intermediate or precursor for Ru_2Si_3 formation, for which $E_{act} \approx 174$ kJ/mol.[16] Ronay and Schad[17] observed similar precursor functionality of Cu_3Si, which was found to lower the formation temperature of $ReSi_2$. Like Ru, B is observed to agglomerate at the Si/Mo interface, as can be seen in Fig. 5.

The B tail in Fig. 5 shows a similar slope for the various B_4C layer thicknesses systems. Small differences can be attributed to ion mixing which is more prominent when more B_4C is present in the system. The B agglomeration is accompanied by a significant B 1*s* electron BE increase in the Mo layer, suggesting that B migration toward the Mo layer is accommodated by MoB_x formation, which stops further B diffusion. A similar mechanism occurs in the multilayer when B_4C diffusion barriers are applied.[3,18–20] Figure 6 shows a ~0.3 nm beam size EELS cross section of a multilayer with five periods of 3.5 nm thick Mo and Si layers on five periods of 3.0 nm thick Mo and Si layers with a 1.0 nm thick B_4C barrier at each interface. The profiles are corrected for the total transmission of the TEM sample, which is much less in Mo than in Si.

The CS-EELS in Fig. 6 reveal highly localized B peaks that are predominantly located in the Mo layers. This means that the B diffuses from both the Mo/Si and Si/Mo interface into the Mo layer, where it can form MoB_x. The in-depth C distribution appears very diffusive with probably a large contribution from the sample preparation. The 16%–84% Mo-on-Si and Si-on-Mo interface widths are 1.08 and 1.24 nm, respectively, compared to 1.75 and 1.50 nm without B_4C. The difference at the Si-on-Mo interface is within the finite resolution and the instrumental error, but the Mo-on-Si interface profits from reduced segregation by application of a B_4C diffusion barrier. HAADF-STEM and EDX analysis with a beam size of ~1.0 nm confirm the observations (Fig. 7), although the barrier layers are not individually identifiable.

In Fig. 7, the B and C presence also appear to reduce layer inhomogeneity and interface diffuseness. In XPS depth profiling studies on Si/Mo multilayers with B_4C diffusion

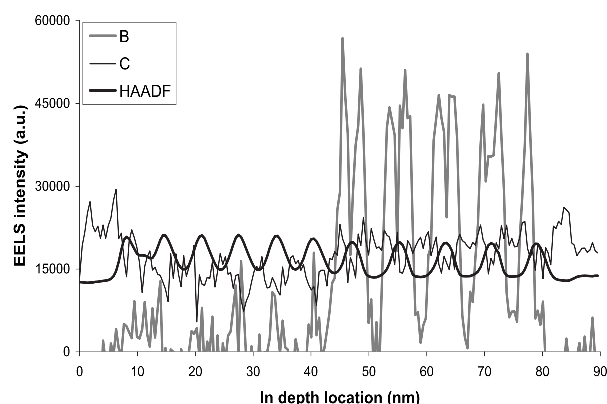

FIG. 6. CS-EELS of a multilayer with five periods of 3.5 nm thick Mo and Si layers on five periods of 3.0 nm thick Mo and Si layers with a 1.0 nm thick B_4C barrier at each interface. Peaks in the HAADF intensity correspond to Mo layers, valleys to Si layers.

Downloaded 07 Sep 2010 to 130.89.22.124. Redistribution subject to AIP license or copyright; see http://jap.aip.org/about/rights_and_permissions

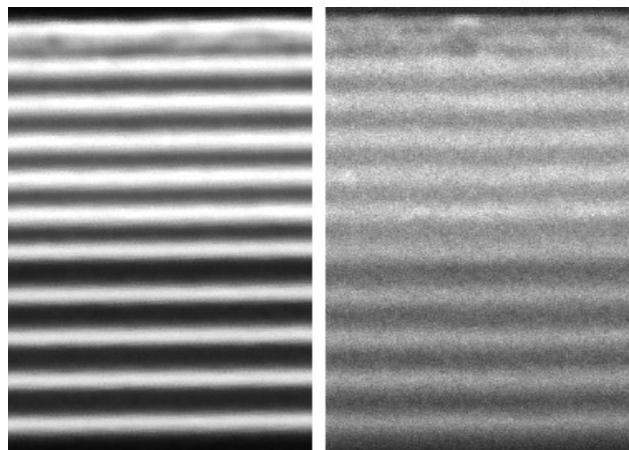

FIG. 7. Cross section EDX (left) and high resolution (<0.3 nm) HAADF-STEM (right) image of a Ru capped $5\times(\mathrm{Mo/Si})$ $5\times(\mathrm{Mo/B_4C/Si/B_4C})$ multilayer.

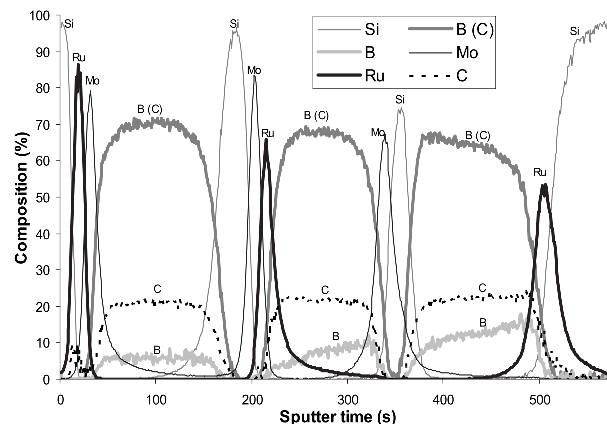

FIG. 8. XPS sputter depth profile of a four material multilayer system with all ad-/substrate layer combinations. B bonded to C is denoted B (c).

barriers, we observe a locally B-rich stoichiometry, while C is more diffused.[3] In the case of Si and B_4C, borides will not spontaneously form due to unfavorable formation enthalpy. Only elemental C that is in equilibrium with B_4C can react with Si to form SiC, with $\Delta H^{\mathrm{for}}{}_{\mathrm{SiC}}=-65$ kJ/mol, considering the chemical equilibrium (K) of compound formation

$$K=e^{-\Delta G^{\mathrm{for}}/RT}=e^{\Delta S^{\mathrm{for}}/R}\cdot e^{-\Delta H^{\mathrm{for}}/RT}, \tag{1}$$

where the ΔS^{for} term covers differences in phase and crystal structure. Since these differences are small for solid-solid interactions occurring at the interface, we take $\Delta G^{\mathrm{for}} \approx \Delta H^{\mathrm{for}}$. B_4C deposition onto Si results in a chemically inactive interface with significant B_4C segregation toward the subsurface to maintain a surface monolayer of Si, of which both the surface free energy and the enthalpy for vacancy formation are lowest.

When B_4C is atomically deposited onto Ru or Mo, the largest kinetic gain is obtained, respectively, by

$$4\mathrm{Ru}+4\mathrm{B}+\mathrm{C}\rightarrow 4\mathrm{RuB}+\mathrm{C}, \quad \text{and} \tag{2}$$

$$6\mathrm{Mo}+4\mathrm{B}+\mathrm{C}\rightarrow 4\mathrm{MoB}+\mathrm{Mo_2C}, \tag{3}$$

with $\Delta H^{\mathrm{for}}{}_{\mathrm{RuB}}=-35$ kJ/mol, $\Delta H^{\mathrm{for}}{}_{\mathrm{MoB}}=-62$ kJ/mol, $\Delta H^{\mathrm{for}}{}_{\mathrm{Mo_2C}}=-46$ kJ/mol,[16] and negligible Ru and Mo lattice energy. This implies formation of RuB via Eq. (2), MoB and Mo_2C via Eq. (3) at the respective interfaces, and negligible B_4C recombination. Surface segregation is not energetically favorable, and the decreasing Ru and Mo atom supply to the surface upon boride formation can favor another stoichiometry. When surface Ru or Mo are finally depleted, B_4C recombination can occur.

The experimental results show reactive interfaces when B_4C is used in multilayer applications. Increased B concentration and B 1s electron BE at the B_4C/Mo interface hint at MoB formation via Eq. (3). Transition metal boride and carbide formation at B_4C interfaces has also been observed by Mogilevsky *et al.*[21] In the experiments, various metal borides and carbides appear to be favored over B_4C, in accordance with the earlier described thermodynamics. To identify the adsorbate/substrate dependency of thin layer growth mechanisms, Fig. 8 shows an XPS sputter depth profile of a four material multilayer with interfaces in all the possible orientations: $\mathrm{Si/Ru/Mo/B_4C/Si/Mo/Ru/B_4C/Mo/Si/B_4C/Ru/Si}$. Ru and Mo layers are 4 nm thick, first and last Si layer is 7 nm, B_4C and other two Si layers is 15 nm.

From the depth profile, it is clear that the sputter rate for B_4C is significantly lower than for Si. Si segregation into B_4C is again visible for B_4C on Si, and to lesser extends for B_4C on Ru and B_4C on Mo, indicating a moderately high surface free energy of the deposited B_4C. Like Ru, diffusion of Mo into a B_4C substrate layer is significant. Clear Mo segregation into Si and relatively sharp B_4C/Mo and Si/Mo interfaces are also visible. For in-depth chemical analysis, Fig. 9 shows the B 1s, C 1s, Ru 3d, Mo 3d, and Si 2p peak shifts from bulk values, superimposed on the depth profile.

Segregation of Mo, similar to Ru, delays B_4C depletion and results in a broad MoB and Mo_2C interlayer. Si 2p, Mo 3d, and Ru 3d electrons all show a considerable upward BE shift when the corresponding materials are deposited onto B_4C, while the shift is much smaller when these materials form the substrate layer for B_4C growth. Significant

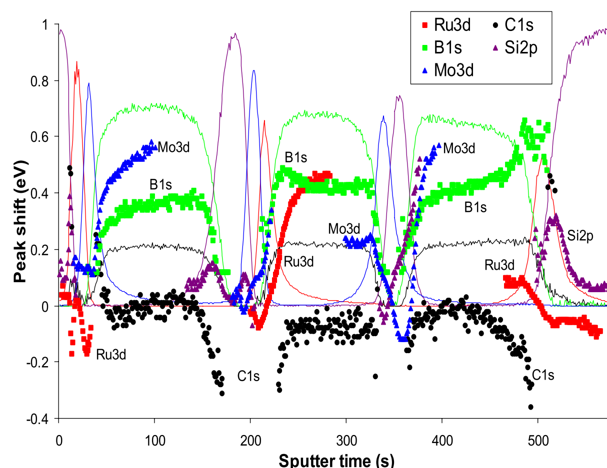

FIG. 9. (Color online) Peak-shifts (dots, superimposed on the depth profile) for Ru 3d, C 1s, B 1s, Si 2p, and Mo 3d as determined by XPS sputter depth profiling. A 0.0 eV peak shift represents binding energies of 280.0, 283.0, 188.0, 99.3, and 227.8 eV for the respective materials.

Downloaded 07 Sep 2010 to 130.89.22.124. Redistribution subject to AIP license or copyright; see http://jap.aip.org/about/rights_and_permissions

B 1*s* peak shifts are observed for B_4C interfaces with Mo and Ru. When Ru is replaced by Y, which has the lowest surface free energy per unit area of the *d*-metals, we observe quite similar diffusion and compound formation. It is remarkable that the BE shifts appear much more adsorbate/substrate than material dependent and that instead of B_4C dissociation, the supply of atoms via segregation is of main influence.

IV. CONCLUSION

Diffusion and compound formation in Ru, Mo, Si, and B_4C layers have been characterized with XPS, CS-EELS, HAADF-STEM, and EDX. Minimization of the surface free energy causes significant B_4C surface segregation into the Si, driving Si toward the surface. The intermixture is not accompanied by chemical activity. The B 1*s*, C 1*s*, and Si 2*p* electron binding energies reveal no SiB and SiC, both species not being kinetically favored over B_4C.

Significant Ru surface segregation and further diffusion into the B_4C and Si layer occur for all B_4C diffusion barrier thicknesses up to 5.0 nm. Ru diffusion coincides with Ru 3*d*, B 1*s*, and C 1*s* electron binding energies that suggest Ru boride formation at the cost of B_4C, particularly for the thickest B_4C layers.

Ru and B diffuse through the Si layer toward the Si/Mo interface front, where agglomeration occurs. This is in accordance with earlier experimental results, which showed Ru agglomeration to also be persistent after annealing. Shifts in the Ru 3*d* and B 1*s* electron binding energies suggest the agglomeration is accompanied by Ru_2Si_3 and MoB formation. Our results confirm earlier conclusions that the Si/Mo interface front acts as a precursor for Ru silicide formation, accommodating Ru migration to minimize the energy. The observations for Ru can be generalized to other *d*-metals including Y, Nb, Rh, and Ir. B agglomeration is found to be accommodated by MoB formation, which is strongly favored over the endothermic SiB formation process and to a lesser extend over formation of RuB.

ACKNOWLEDGMENTS

This work is part of the FOM Industrial Partnership Programme I10 ("XMO") which is carried out under contract with Carl Zeiss SMT AG, Oberkochen and the "Stichting voor Fundamenteel Onderzoek der Materie (FOM)," the latter being financially supported by the "Nederlandse Organisatie voor Wetenschappelijk Onderzoek (NWO)." The authors wish to thank Dr. J.G.M. van Berkum of Philips Research for the CS-EELS, HAADF-STEM, and EDX measurements.

[1]T. Young, Philos. Trans. R. Soc. London **95**, 65 (1805).
[2]H. Roder, R. Schuster, and K. Kern, Phys. Rev. Lett. **71**, 13 (1993).
[3]I. Nedelcu, R. W. E. van de Kruijs, A. E. Yakshin, F. Bijkerk, Appl. Opt. **48**, 155 (2009).
[4]T. Tsarfati, E. Zoethout, R. W. E. van de Kruijs, and F. Bijkerk, J. Appl. Phys. **105**, 064314 (2009).
[5]L. E. Klebanoff, M. E. Malinowski, P. A. Grunow, W. M. Clift, C. Steinhaus, A. H. Leung, and S. J. Haney, Proc. SPIE **4343**, 342 (2001).
[6]T. Tsarfati, E. Zoethout, R. W. E. van de Kruijs, F. Bijkerk, Surf. Sci. **603**, 1041 (2009).
[7]S. Bâjt, J. B. Alameda, T. W. Barbee, Jr., W. M. Clift, J. A. Folta, B. Kaufmann, and E. A. Spiller, Opt. Eng. **41**, 1797 (2002).
[8]E. Louis, H.-J. Voorma, N. B. Koster, L. Shmaenok, F. Bijkerk, R. Schlatmann, J. Verhoeven, Yu. Ya. Platonov, G. E. van Dorssen, and H. A. Padmore, Microelectron. Eng. **23**, 215 (1994).
[9]A. E. Yakshin, E. Louis, P. C. Görts, E. L. G. Maas, and F. Bijkerk, Physica B **283**, 143 (2000).
[10]R. W. E. van de Kruijs, E. Louis, A. E. Yakshin, P. Suter, E. Zoethout, F. Bijkerk, S. Müllender, H. Enkisch, H. Trenkler, M. Wedowski, M. Weiss, B. Mertens, B. Wolschrijn, R. Jansen, A. Duisterwinkel, A. van de Runstraat, R. Klein, S. Plőger, and F. Scholze, Proceedings of the 2nd International EUV Lithography Symposium, 2003, Antwerp (unpublished).
[11]J. F. Ziegler and J. P. Biersack, Computer code SRIM-2008 program package, http://www.srim.org
[12]S. Tanuma, C. J. Powell, and D. R. Penn, Surf. Interface Anal. **17**, 911 (1991).
[13]A.-L. Barabási, Phys. Rev. Lett. **70**, 26 (1993).
[14]B. M. Clemens, W. D. Nix, and V. Ramaswamy, J. Appl. Phys. **87**, 6 (2000).
[15]T. Tsarfati, E. Zoethout, R. W. E. van de Kruijs, and F. Bijkerk, Opt. Lett. (submitted).
[16]F. R. de Boer, R. Boom, W. C. M. Mattens, A. R. Miedema, and A. K. Niessen, *Cohesion in Metals: Transition Metal Alloys* (North-Holland, Amsterdam, 1988).
[17]M. Ronay and R. G. Schad, Phys. Rev. Lett. **64**, 2042 (1990).
[18]A. Patelli, V. Rigato, G. Salmaso, N. J. M. Carvalho, J. Th. M. De Hosson, E. Bontempi, and L. E. Depero, Surf. Coat. Technol. **201**, 143 (2006).
[19]L. G. Jacobsohn, R. D. Averitt, M. Nastasi, J. Vac. Sci. Technol. A **21**, 1639 (2003).
[20]T. Böttger, D. C. Meyer, P. Paufler, S. Braun, M. Moss, H. Mai, E. Beyer, Thin Solid Films **444**, 165 (2003).
[21]P. Mogilevsky, E. Y. Gutmanas, I. Gotman, and R. Telle, J. Eur. Ceram. Soc. **15**, 527 (1995).

Downloaded 07 Sep 2010 to 130.89.22.124. Redistribution subject to AIP license or copyright; see http://jap.aip.org/about/rights_and_permissions